A new auto-coherent bias dependent charge model for MESFETs and HEMTs

S. Valkov, D. Derzkii, F. Temcamani, P. Pouvil

ENSEA, Laboratoire EMO, 6 Avenue du Ponceau, 95014 Cergy Pontoise cedex, France

Abstract

A nonlinear model of MESFETs and HEMTs capacitances suitable for implementation in commercial circuit design software is presented. The model is based upon the determination of the nonlinear bias dependent charge equations. A comparison is made between capacitance values coming from PHEMT characterization and capacitance values derived from the model.

Introduction

Commercial design software require accurate nonlinear capacitance models based on charge bias dependent equations. Usually, the quasi-static approch is applied to find these equations [1]. The capacitance instantaneous values are assumed to be equal to their incremental values extracted from S parameters small-signal measurements at each operating point.

The intrinsic equivalent circuit for the displacement current part of a MESFET or a HEMT is shown in Fig. 1. The determination of both large signal gate Q_g and drain Q_d charges from the three small-signal bias dependent capacitance has been proposed in several publications.

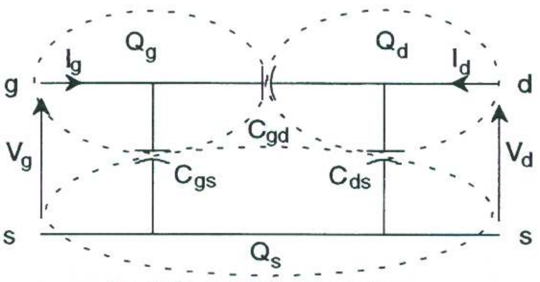

Fig. 1: Current displacement scheme.

In [2], [3], [4] and [5], only C_{gs} is considered as dependent of V_g and V_d. In [6] and [7], C_{ds} is considered as bias independent and the gate charge Q_g is artificially divided into two non-physical charges Q_{gs} and Q_{gd} corresponding to C_{gs} and C_{gd} and in [8], independent empirical formulas for Q_g and Q_d are given. These solutions ensure neither the Y matrix reciprocity for the equivalent circuit shown in Fig. 1, nor the coherence between Q_g and Q_d. This introduces convergence problems which may occur during the circuit simulations and in fact, all of the three capacitances are nonlinear [9], [10], [11], [12].

The aim of this work is to find coherent large signal analytic expresssions for Q_g, Q_d, C_{gs}, C_{gd} and C_{ds}.

Theoretical

Assuming that $Q_g(V_g,V_d)$ and $Q_d(V_g,V_d)$ are the gate and drain charges at the operating point (V_g,V_d), their complete differentials are :

$$dQ_g = \frac{\partial Q_g}{\partial V_g} dV_g + \frac{\partial Q_g}{\partial V_d} dV_d \qquad (1)$$

$$dQ_d = \frac{\partial Q_d}{\partial V_g} dV_g + \frac{\partial Q_d}{\partial V_d} dV_d \qquad (2)$$

The displacement currents are given by :

$$I_g = \frac{dQ_g}{dt} = C_{11}\frac{dV_g}{dt} + C_{12}\frac{dV_d}{dt} \qquad (3)$$

$$I_d = \frac{dQ_d}{dt} = C_{21}\frac{dV_g}{dt} + C_{22}\frac{dV_d}{dt} \qquad (4)$$

C_{ij} are the incremental capacitances of the two-port shown in Fig. 1.

In the frequency domain (3) and (4) give :

$$I_g = j\omega C_{11}V_g + j\omega C_{12}V_d \qquad (5)$$

$$I_d = j\omega C_{21}V_g + j\omega C_{22}V_d \qquad (6)$$

According to the Y matrix of Fig. 1, we obtain :

$$C_{11} = \left.\frac{\partial Q_g}{\partial V_g}\right|_{V_d} = C_{gs} + C_{gd} \qquad (7)$$

$$C_{12} = \left.\frac{\partial Q_g}{\partial V_d}\right|_{V_g} = -C_{gd} \qquad (8)$$

$$C_{21} = \left.\frac{\partial Q_d}{\partial V_g}\right|_{V_d} = -C_{gd} \qquad (9)$$

$$C_{22} = \left.\frac{\partial Q_d}{\partial V_d}\right|_{V_g} = C_{ds} + C_{gd} \qquad (10)$$

It is obvious that analytic expressions for $C_{gs}(V_g,V_d)$, $C_{gd}(V_g,V_d)$ and $C_{ds}(V_g,V_d)$ must not only fit accurately with data but they must satisfy the system (7) to (10).

Analytical expressions for charges and capacitances

The best polynimial expression for C_{gd} obtained by a free data fitting is :

$$\begin{aligned} C_{gd} &= c_{00} + c_{01}V_d + c_{02}V_d^2 + c_{03}V_d^3 + c_{04}V_d^4 \\ &+ c_{05}V_d^5 + c_{10}V_g + c_{11}V_gV_d + c_{12}V_gV_d^2 \\ &+ c_{13}V_gV_d^3 + c_{14}V_gV_d^4 \end{aligned} \qquad (11)$$

Putting C_{gd} from (11) into (8) and (9) and integrating, we deduce :

$$\begin{aligned} Q_g &= x_{01}V_d + x_{02}V_d^2 + x_{03}V_d^3 + x_{04}V_d^4 + x_{05}V_d^5 \\ &+ x_{06}V_d^6 + x_{11}V_gV_d + x_{12}V_gV_d^2 + x_{13}V_gV_d^3 \\ &+ x_{14}V_gV_d^4 + x_{15}V_gV_d^5 \\ &+ \left(x_{10}V_g + x_{20}V_g^2 + x_{30}V_g^3 + x_{40}V_g^4 + x_{50}V_g^5\right) \end{aligned} \qquad (12)$$

$$\begin{aligned} Q_d &= y_{10}V_g + y_{11}V_gV_d + y_{12}V_gV_d^2 + y_{13}V_gV_d^3 \\ &+ y_{14}V_gV_d^4 + y_{15}V_gV_d^5 + y_{20}V_g^2 + y_{21}V_g^2V_d \\ &+ y_{22}V_g^2V_d^2 + y_{23}V_g^2V_d^3 + y_{24}V_g^2V_d^4 + \\ &\left(\begin{array}{l} y_{01}V_d + y_{02}V_d^2 + y_{03}V_d^3 + y_{04}V_d^4 + y_{05}V_d^5 \\ + y_{06}V_d^6 + y_{07}V_d^7 + y_{08}V_d^8 \end{array}\right) \end{aligned} \qquad (13)$$

Integrated constants are represented by the quantities included in the brackets. Their degrees have been found to be optimal.

Placing Q_g and Q_d from (12) and (13) and C_{gd} from (11) into (7) and (10), we obtain :

$$\begin{aligned} C_{gs} &= a_{00} + a_{01}V_d + a_{02}V_d^2 + a_{03}V_d^3 + a_{04}V_d^4 \\ &+ a_{05}V_d^5 + a_{10}V_g + a_{11}V_gV_d + a_{12}V_gV_d^2 \\ &+ a_{13}V_gV_d^3 + a_{14}V_gV_d^4 + a_{20}V_g^2 + a_{30}V_g^3 \\ &+ a_{40}V_g^4 \end{aligned} \qquad (14)$$

$$\begin{aligned} C_{ds} &= b_{00} + b_{01}V_d + b_{02}V_d^2 + b_{03}V_d^3 + b_{04}V_d^4 \\ &+ b_{05}V_d^5 + b_{06}V_d^6 + b_{07}V_d^7 + b_{10}V_g + b_{11}V_gV_d \\ &+ b_{12}V_gV_d^2 + b_{13}V_gV_d^3 + b_{14}V_gV_d^4 + b_{20}V_g^2 \\ &+ b_{21}V_g^2V_d + b_{22}V_g^2V_d^2 + b_{23}V_g^2V_d^3 \end{aligned} \qquad (15)$$

Polynomial coefficients determination

The relations between the charge polynomial coefficients x_{ij}, y_{ij} and the capacitance coefficients a_{ij}, b_{ij}, c_{ij} is done by a system of 42 linear equations which are easily deduced from (7), (8) and (10) to (15). However, 18 of these equations are redundant. This is traduced by an interdependence of some capacitance coefficients as follows :

$$\begin{gathered} a_{01} + c_{10} + c_{01} = 0 \\ a_{11} + c_{11} = 0 \\ 2a_{02} + c_{11} + 2c_{02} = 0 \\ a_{12} + c_{12} = 0 \\ 3a_{03} + c_{12} + 3c_{03} = 0 \\ a_{13} + c_{13} = 0 \\ 4a_{04} + c_{13} + 4c_{04} = 0 \\ a_{14} + c_{14} = 0 \\ 5a_{05} + c_{14} + 5c_{05} = 0 \\ b_{10} + c_{10} + c_{01} = 0 \\ 2b_{20} + c_{11} = 0 \\ b_{11} + c_{11} + 2c_{02} = 0 \\ b_{21} + c_{12} = 0 \\ b_{12} + c_{12} + 3c_{03} = 0 \\ 2b_{22} + 3c_{13} = 0 \\ b_{13} + c_{13} + 4c_{04} = 0 \\ b_{23} + 2c_{14} = 0 \\ b_{14} + c_{14} + 5c_{05} = 0 \end{gathered} \qquad (16)$$

Taking into account these redundances, the optimal values of a_{ij}, b_{ij} and c_{ij} could be found by minimizing the error function :

$$\begin{aligned} f = \sum_i &\left[\begin{array}{l} \left(C_{gse_i} - C_{gs_i}\right)^2 + \left(C_{gde_i} - C_{gd_i}\right)^2 \\ + \left(C_{dse_i} - C_{ds_i}\right)^2 \end{array}\right] \\ &+ g_1\left(a_{01} + c_{10} + c_{01}\right) + g_2\left(a_{11} + c_{11}\right) \\ &+ \cdots + g_{18}\left(b_{14} + c_{14} + 5c_{05}\right) \end{aligned} \qquad (17)$$

C_{gse}, C_{gde}, C_{dse} are the experimental extracted capacitance values and C_{gs}, C_{gd}, C_{ds}, the literal capacitance values coming from (11), (14) and (15). g_1 to g_{18} are Lagrange multipliers [13].

The 35 charge coefficients x_{ij} and y_{ij} are calculated from the 24 non redundant equations and from 11 equations coming from (8) and (9) in respect of the Y matrix reciprocity :

$$\begin{gathered} y_{10} = x_{01} \\ 2y_{20} = x_{11} \\ y_{11} = 2x_{02} \\ y_{21} = x_{12} \\ y_{12} = 3x_{03} \\ 2y_{22} = 3x_{13} \\ y_{13} = 4x_{04} \\ y_{23} = 2x_{14} \\ y_{14} = 5x_{05} \\ 2y_{24} = 5x_{15} \\ y_{15} = 6x_{06} \end{gathered} \qquad (18)$$

Results

The voltage capacitance dependences (x10^{-13}Farad) for C_{gs}, C_{gd} and $C_d = C_{ds} + C_{pd}$ obtained by a free fitting of the experimental data (a) and by derivating the charges (b) are shown in Fig. 2 to Fig. 4, for a 0.5 µm gate length and 2x50 µm gate width PHEMT. C_{pd} is the bias independent electrostatic drain capacitance value.

V_g and V_d are the intrinsic potential taking into account ohmic losses in the parasitic source and drain access resistances.

The absolute average errors in comparison with the experimental data are given in table 1.

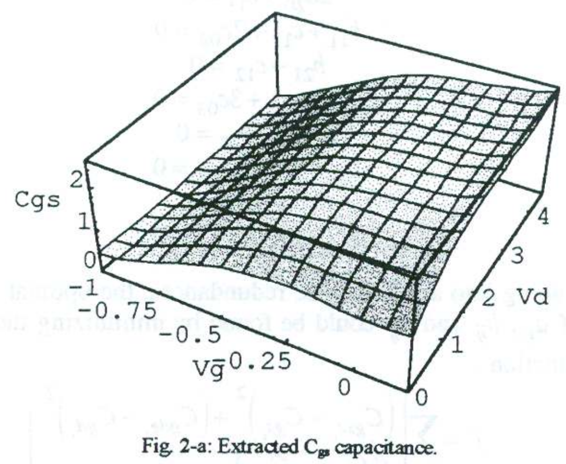

Fig. 2-a: Extracted C_{gs} capacitance.

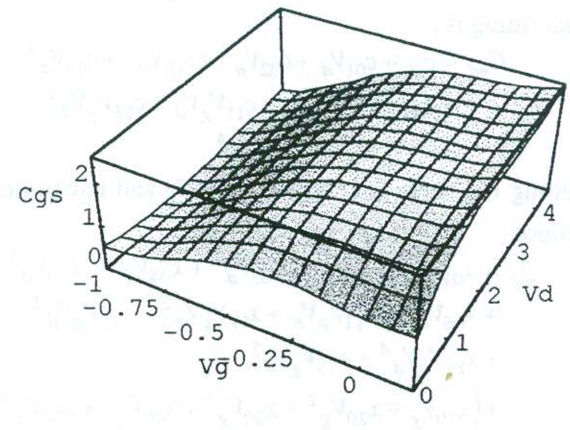

Fig. 2-b: Modeled C_{gs} capacitance.

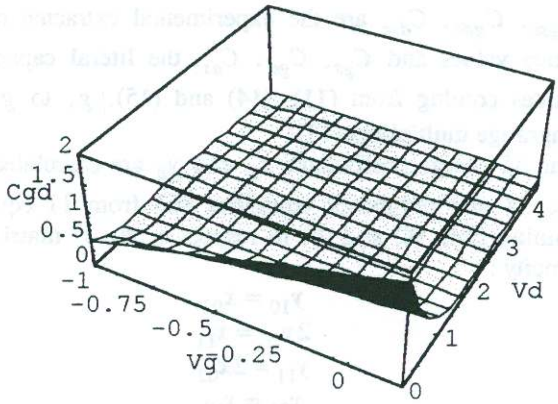

Fig. 3-a: Extracted C_{gd} capacitance.

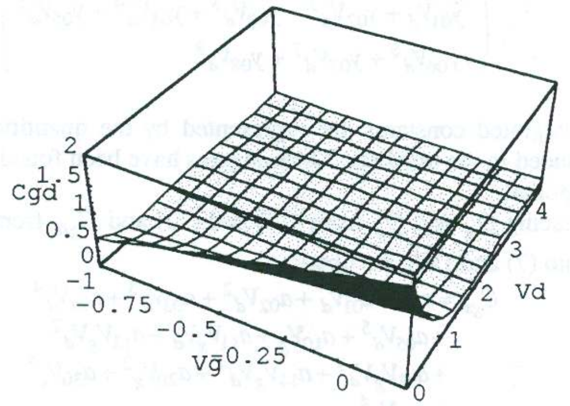

Fig. 3-b: Modeled C_{gd} capacitance.

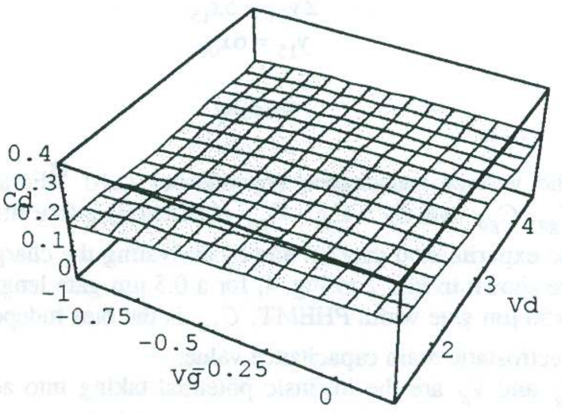

Fig. 4-a: Extracted $C_d = C_{ds} + C_{pd}$ capacitance.

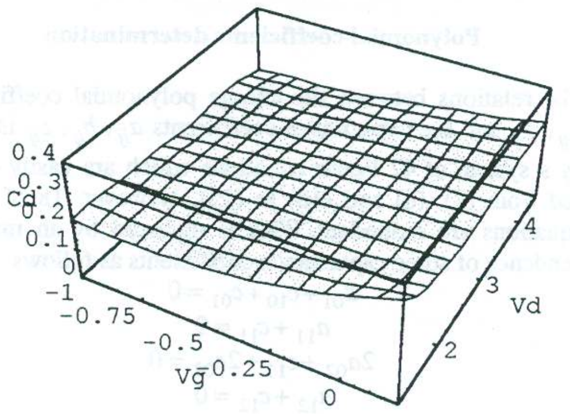

Fig. 4-b: Modeled $C_d = C_{ds} + C_{pd}$ capacitance.

Table 1: Comparison between errors.

Capacitance	C_{gs}	C_{gd}	$C_{ds}+C_{pd}$
Fit method error	4.23%	9.85%	1.61%
Derivate method error	4.50%	10.60%	5.40%

S parameters are measured on wafer by using a LRM calibrage on the frequency range 0.5 GHz to 40 GHz.
Similar results are obtained for a 4x100 µm gate width PHEMT.
The charge model was implemented in the Hewlett-Packard Microwave Design System software (MDS) as a Symbolically Defined Device (SDD).

Acknowledgment

The authors greatly acknowledge R. Leblanc and B. Byzery of Philips Microwave Limeil Company for their interest in this work and for PHEMT supplies.

References

[1] C. Rauscher, H. A. Willing, "Simulation of nonlinear microwave FET performance using a quasi-static model", *IEEE Trans. MTT*, Vol. MTT-27, no.10, pp. 834-840, Oct. 1979.

[2] R. A. Pucel, H. A. Haus, H. Statz, "Signal and noise properties of GaAs microwave field effect transistors", *Advances in Electronics and Electron Physics*, Vol. 38, pp. 195-265, Ed. L. Marton, Academic Press, New York, 1975.

[3] A. Materka, T. Kacprzak, "Computer calculation of large signal GaAs FET amplifier characteristics", *IEEE Trans. MTT*, Vol. MTT-33, no.2, pp. 129-135, Feb. 1985.

[4] W. R. Curtice, "GaAs MESFET modeling and nonlinear CAD", *IEEE Trans. MTT*, Vol. MTT-36, no.2, pp. 220-230, Feb. 1988.

[5] Y. Tajima, B. Wrona, K. Mishima, "GaAs FET large signal model and its application to circuit designs", *IEEE Trans. Elec. Dev.*, Vol. ED-28, no.2, pp. 171-175, Feb. 1981.

[6] H. Statz, P. Newman, I. W. Smith, R. A. Pucel, H. A. Haus, "GaAs FET device and circuit simulation in SPICE", *IEEE Trans. Elec. Dev.*, Vol. ED-34, no.2, pp. 160-169, Feb. 1987.

[7] G. George, J. R. Hauser, "An analytic model for MODFET capacitance-voltage characteristics", *IEEE Trans. Elec. Dev.*, Vol. 37, no.5, pp. 1193-1198, May. 1990.

[8] V. Rizzoli, A. Constanzo, A. Neri, "An advanced empirical model for use in nonlinear simulation", *22 Euro. Microwave Conference* Proc., pp. 1103-1108, Espoo, Finland, 1992.

[9] R. Anholt, S. Swirhun, "Measurement and analysis of GaAs MESFET parasitic capacitances", *IEEE Trans. MTT*, Vol. MTT-39, no.7, pp. 1247-1251, July, 1991.

[10] T. H. Chen, M. S. Shur, "A capacitance model for GaAs MESFET's", *IEEE Trans. Elec. Dev.*, Vol. ED-12, no.5, pp. 883-891, May. 1985.

[11] I. Corbella, J. M. Legido, G. Naval, "Instantaneous model of a MESFET to use in linear and nonlinear circuit simulations", *IEEE Trans. MTT*, Vol. 40, no.7, pp. 1410-1421, July, 1992.

[12] J. Rodriguez-Tellez, K. A. Mezher, O. M. Conde-Portilla, J. C. Luengo-Patrocinio, "A highly accurate microwave nonlinear MESFET model", *Microwave Journal*, pp. 280-285, May, 1993.

[13] G. A. Korn, T. M. Korn, *"Mathematical handbook for scientists and engineers"*, Ed. McGraw-Hill, New York, 1961.